JOURNAL OF PROPULSION AND POWER
Vol. 26, No. 6, November–December 2010

Technical Notes

Discharge Coefficient of Expanded Exit Holes for Film Cooling of Turbine Blades

Fariborz Forghan
Advanced Consultant Engineering, Mansfield, Massachusetts 02048
and
Uichiro Narusawa and Hameed Metghalchi*
Northeastern University, Boston, Massachusetts 02115

DOI: 10.2514/1.48694

Nomenclature

A	=	flow cross-sectional area
A_e	=	exit area
A^*	=	throat area
C_D	=	discharge coefficient
$C_{D,C}$	=	discharge coefficient of choked flow
$C_{D,\mathrm{NC}}$	=	discharge coefficient of nonchoked flow
M	=	Mach number
$M_{e,\mathrm{sub}}$	=	subsonic Mach number at the exit
M_{throat}	=	Mach number at the throat
$\dot{m}_{\mathrm{act}}$	=	actual mass-flow rate
$\dot{m}_C$	=	mass-flow rate of choked isentropic flow
$\dot{m}_{\mathrm{isen}}$	=	isentropic mass-flow rate
$\dot{m}_{\mathrm{NC}}$	=	mass-flow rate of nonchoked isentropic flow
P	=	pressure
P_b	=	backpressure
P_{bc}	=	critical backpressure for the onset of choked flow
$P_\circ$	=	stagnation (total) pressure
R	=	mass-based gas constant
$T_\circ$	=	stagnation (total) temperature
γ	=	specific heat ratio

I. Introduction

GAS turbine blades, being exposed to high-temperature combustion gases, are cooled by gas flow fed through holes that are made along the blades (film-cooling holes of turbine blades) [1–8]. Each hole for film cooling may be regarded as a (convergent) divergent nozzle to be referred to as an expanded exit hole (EEH). Mass- and momentum-flow rates of the coolant at the exit of an EEH determine how well the coolant shields the blade surface from the mainstream hot gas. For specified total (stagnation) pressure $P_\circ$ and total temperature $T_\circ$, the effectiveness of film cooling is affected by a magnitude of the backpressure (equal to the pressure at the exit of an EEH) P_b and such geometric conditions as the minimum cross-sectional area (equal to the throat area) A^* and the exit area A_e. As is the case with any other type of flow through a restriction of complex geometry [9], a discharge coefficient is defined for an EEH [10–26] as

$$C_D = \frac{\dot{m}_{\mathrm{act}}}{\dot{m}_{\mathrm{isen}}} \tag{1}$$

where $\dot{m}_{\mathrm{act}}$ is the actual mass-flow rate through an EEH, and $\dot{m}_{\mathrm{isen}}$ is the mass-flow rate through an EEH under isentropic flow conditions; the former is measured for a specified EEH, while the latter is evaluated theoretically for given reservoir and geometric conditions of an EEH. The magnitude of C_D should be less than unity, because such irreversible effects as gas expansion/contraction and viscous shear cause deviations from isentropic conditions. However, various experimental reports in the past maintain that C_D may exceed 1.0 for an EEH under certain conditions [18,22,25]. This Note proposes a new definition of C_D that is consistent with the flow structure within an EEH.

II. Theoretical Background

To analyze an EEH, we consider a steady one-dimensional isentropic flow of an ideal gas (specific heat ratio $\gamma =$ constant) in a converging–diverging nozzle, with the throat being the location of a minimum-flow cross section.

With $P_b < P_\circ$, the flow is subsonic if the Mach number at the throat (M_{throat}) is less than unity. The subsonic flow accelerates (decelerates) in the converging (diverging) section as the static pressure P decreases (increases) in the converging (diverging) section. On the other hand, the flow is choked if the sonic condition is reached at the throat (i.e., $M_{\mathrm{throat}} = 1$). Under the choked conditions in which signals generated downstream of the throat fail to reach upstream, the entire flow in the upstream converging section of the nozzle is insensitive to flow conditions downstream of the throat (i.e., the diverging section), implying that the streamwise pressure distribution in the converging section remains the same even as P_b is further reduced. Accordingly, the isentropic mass-flow rate $\dot{m}_{\mathrm{isen}}$ that appears in the denominator of Eq. (1) is different between the nonchoked flow ($\dot{m}_{\mathrm{isen}} \equiv \dot{m}_{\mathrm{NC}}$) and the choked flow ($\dot{m}_{\mathrm{isen}} \equiv \dot{m}_C$). The mass-flow rate of nonchoked isentropic flow $\dot{m}_{\mathrm{NC}}$ may be expressed in terms of P_b and the exit cross section A_e as

$$\dot{m}_{\mathrm{NC}} = P_\circ \left(\frac{\gamma}{RT_\circ}\right)^{1/2} A_e \left(\frac{P_b}{P_\circ}\right)^{\frac{\gamma+1}{2\gamma}} \left[\left(\frac{2}{\gamma-1}\right)\left(\left(\frac{P_\circ}{P_b}\right)^{\frac{\gamma-1}{\gamma}} - 1\right)\right]^{\frac{1}{2}} \tag{2}$$

The isentropic flow under choked conditions results in

$$\dot{m}_C = P_\circ \left(\frac{\gamma}{RT_\circ}\right)^{1/2} A^* \left(\frac{2}{\gamma+1}\right)^{\frac{\gamma+1}{2(\gamma-1)}} \tag{3}$$

It should be noted that $\dot{m}_C$ is independent of the magnitude of the backpressure. In summary, flow through a (converging) diverging nozzle is subsonic with $\dot{m}_{\mathrm{isen}} = \dot{m}_{\mathrm{NC}}$ if $P_{\mathrm{bc}} < P_b < P_\circ$, and it is choked with $\dot{m}_{\mathrm{isen}} = \dot{m}_C$ if $P_b \le P_{\mathrm{bc}}$.

The critical backpressure P_{bc} in the two relations shown above may be defined as the backpressure, below which the flow is choked at the throat. Its magnitude for an isentropic flow through EEH with the area ratio A_e/A^* may be found from Eqs. (4) and (5); the former is a relation between the area ratio A_e/A^* and the subsonic Mach number at the exit ($M_{e,\mathrm{sub}}$), and the latter is a relation between a pressure ratio of P_o/P_{bc} and $M_{e,\mathrm{sub}}$:

$$\frac{A_e}{A^*} = \frac{(1 + \frac{\gamma-1}{2} M_{e,\mathrm{sub}}^2)^{(\gamma+1)/(2(\gamma-1))}}{M_{e,\mathrm{sub}} (\frac{\gamma+1}{2})^{(\gamma+1)/(2(\gamma-1))}} \tag{4}$$

Received 28 December 2009; revision received 14 July 2010; accepted for publication 24 July 2010.

*Mechanical and Industrial Engineering Department; metghalchi@coe.neu.edu (Corresponding Author).

$$\frac{P_\circ}{P_b} = \left(1 + \frac{\gamma - 1}{2} M_{e,\text{sub}}^2\right)^{\gamma/(\gamma-1)} \tag{5}$$

Then the definition of the discharge coefficient C_D becomes

$$C_{D,\text{NC}} (\equiv C_D(P_{\text{bc}} < P_b < P_\circ)) = \frac{\dot{m}_{\text{act}}}{\dot{m}_{\text{NC}}} \tag{6a}$$

$$C_{D,C} (\equiv C_D(0 < P_b < P_{\text{bc}})) = \frac{\dot{m}_{\text{act}}}{\dot{m}_C} \tag{6b}$$

with

$$C_{D,C} = C_{D,\text{NC}} \frac{\dot{m}_{\text{NC}}}{\dot{m}_C} \tag{7}$$

The factor $\dot{m}_{\text{NC}}/\dot{m}_C$ is a function of A_e/A^*, $P_\circ/P_b$, and γ, as seen from Eqs. (2) and (3).

III. Discussion of Previous Experimental Results

$C_{D,\text{NC}}$ of Eq. (6a) is valid for flow that is not choked at the throat, as subsonic flow prevails throughout EEH. However, when choked at the throat, the flow is accompanied by shock waves or expansion waves downstream of the throat, requiring $C_{D,C}$ of Eq. (6b) as the definition of the discharge coefficient.

Figure 1 plots $P_\circ/P_{\text{bc}}$ vs A_e/A^*, obtained by solving Eqs. (4) and (5) for $\gamma = 1.4$. (Results are similar for gases with $\gamma \neq 1.4$.) If the magnitude of $P_\circ/P_b$ (ratio of the total pressure to the actual backpressure) is above the $P_\circ/P_{\text{bc}} - A_e/A^*$ curve, the flow is choked at the throat for a specified area ratio A_e/A^*. In this case, $C_{D,C}$ of Eq. (6b) is the correct form for the discharge coefficient. If, on the other hand, $P_\circ/P_b$ falls below the $P_\circ/P_{\text{bc}} - A_e/A^*$ curve, the discharge coefficient should be based on Eq. (6a). In relation to limiting cases of the curve in Fig. 1, there are two extreme cases of isentropic flow through EEH, in which a pressure change is induced by an area change: the case of an orifice (i.e., $A_e/A^* = 1$) and the case of a large area change in the diverging section (i.e., $A_e/A^* \to \infty$). For the case of an orifice, Eqs. (4) and (5) predict that flow becomes choked (i.e., $M_{e,\text{sub}} = 1$) at

$$\frac{P_\circ}{P_{\text{bc}}} \approx 1.893 \left(\left(\frac{\gamma + 1}{2}\right)^{\frac{\gamma}{\gamma-1}},\ \gamma = 1.4. \right) \tag{8}$$

For the second case of a large area variation, on the other hand, the flow becomes choked for a small pressure difference between P_o and P_b:

$$\frac{P_\circ}{P_{\text{bc}}} = 1 + \varepsilon \qquad (0 < \varepsilon \ll 1) \quad \text{as } A_e/A^* \to \infty \tag{9}$$

Figure 2 shows experimental results of C_D vs $P_\circ/P_b$ by Forghan [15]. Experimental conditions are flow of air through an inclined conical EEH, cone angle of 8 deg, inclination angle at cone centerline

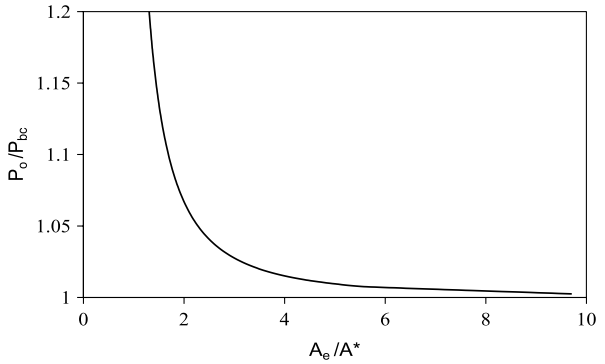

Fig. 1 Critical pressure ratio (total to critical backpressure) as a function of exit-to-throat area ratio.

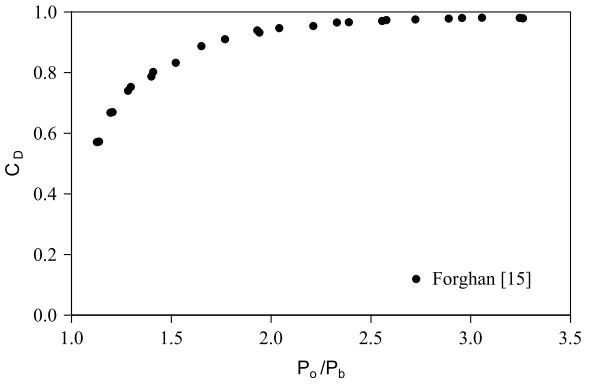

Fig. 2 Discharge coefficient of conical holes for turbine blade film cooling of Forghan [15].

of 35 deg from parallel plate surfaces ($t = 31$ mm), $A_e/A^* = 3.42$, and minimum hole diameter of 8.1 mm.

Figure 1 confirms that all measured data points in Fig. 2 are under choked conditions ($P_\circ/P_b \geq 1.1$ with $P_\circ/P_{\text{bc}} \approx 1.021$ at $A_e/A^* = 3.42$) with C_D evaluated from Eq. (6b) accordingly.

The discharge coefficient of an EEH for film cooling has also been studied extensively by other investigators [10,17,19,20,23,25,26]. Their analyses are based on Eq. (6a), with no discussion on a possible presence of shock waves or expansion waves downstream of the throat. Two cases from previous reports containing sufficient information for our reevaluation of C_D (shown in Figs. 3 and 4) are as follows:

1) A data set for a normal (90 deg) flared film-cooling hole presented in Fig. 6(a) of Hay and Lampard [16] with $A_e/A^* = 4.8$ and $P_\circ/P_b \geq 1.08$ is shown in Fig. 3.

2) A data set for a laid-back fan-shaped hole presented in Fig. 8 of Gritsch et al. [20] with $A_e/A^* = 3.9$ and $P_\circ/P_b \geq 1.04$ is shown in Fig. 4.

Figure 1 predicts P_o/P_{bc} ($A_e/A^* = 3.9$) ≈ 1.015 for case 1 and P_o/P_{bc} ($A_e/A^* = 4.8$) ≈ 1.010 for case 2, thus confirming that the flow is choked over the entire experimental ranges. In analyzing these two data sets, the values of the discharge coefficient $C_{D,\text{NC}}$ at $P_\circ/P_b$ are read from their figures. Then $\dot{m}_{\text{NC}}$ [from Eq. (2)], $\dot{m}_C$ [from Eq. (3)], and $\dot{m}_{\text{act}}$ ($C_{D,\text{NC}}\dot{m}_{\text{NC}}$) are evaluated for each data point to obtain the relation $C_{D,C}$ ($\dot{m}_{\text{act}}/\dot{m}_C$) vs $P_\circ/P_b$.

In Figs. 3 and 4, unfilled symbols are the reported data points obtained from [16,20], and filled symbols are the discharge coefficient calculated from Eq. (6b). It is important to note that the magnitude of $P_\circ/P_{\text{bc}}$ is very close to unity for the area ratio $A_e/A^* \geq 3$ (see Fig. 1). For example, at $A_e/A^* = 3$, the flow is choked for $P_\circ/P_b \geq 1.027$, while at $A_e/A^* = 4$, the flow is choked for $P_\circ/P_b \geq 1.015$. For both cases 1 and 2 the measured range of the

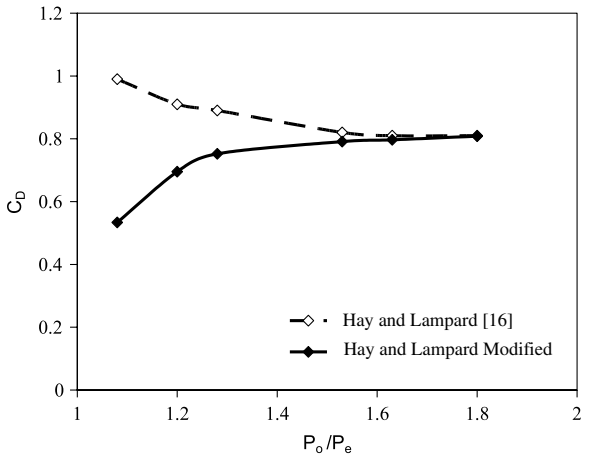

Fig. 3 Discharge coefficient of Hay and Lampard [16] and its modified values based on current model.

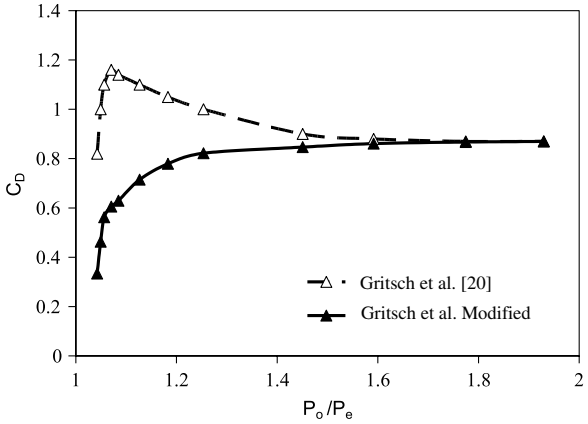

Fig. 4 Discharge coefficient of Gritsch et al. [20] and its modified values based on current model.

pressure ratio $P_\circ/P_b$ is significantly greater than $P_\circ/P_{bc}$. For $P_b \approx P_{bc}$, actual flow may not be under choked conditions even when the isentropic relation of Fig. 1 predicts choked conditions; however, the critical backpressure found for isentropic flow should be used as part of the C_D definition. It should also be noted that once the flow is choked, there are two values of the backpressure (subsonic and supersonic conditions at the exit, respectively) that satisfy the isentropic formulation. The critical backpressure P_{bc} corresponds to the subsonic backpressure as onset of the choked conditions. Equation (6a), if used for C_D evaluations as practiced by all previous studies on EEHs [10,17,19,20,23,25,26], fails for the backpressure below P_{bc}, because 1) one-dimensional isentropic solutions do not exist in this backpressure region, and 2) irreversible shock or expansion waves are generated downstream of the throat for real (nonisentropic or irreversible) flow. It is also mentioned here that the choked mass-flow rate in Eq. (6b) is derived from isentropic flow conditions, even though the flow downstream of the throat is irreversible due to the presence of shock or expansion waves. The original results (unfilled data points) in Figs. 3 and 4 indicate the discharge coefficient to be high, exceeding or very close to 1.0 in the region near $P_\circ/P_b \approx 1.1$. Probable causes as well as various reasons for the high values of C_D had been extensively discussed before [6,18,22,23,25,26]. The discharge coefficient after correction (filled symbols), on the other hand, increases monotonically with the pressure ratio without violating the requirement of $C_D < 1.0$ under real flow conditions. In fact, C_D variations are similar between the curve in Fig. 2 and the two curves after correction (filled symbols) in Figs. 3 and 4. The (normal or oblique) shock front moves downstream of an EEH as the pressure ratio $P_\circ/P_b$ increases beyond $P_\circ/P_{bc}$, finally being pushed out of an EEH to generate expansion waves. It is interesting to see that although the irreversibility associated with the entropy production within a shock wave (with its thickness of the order of microns) increases as its location moves downstream, the discharge coefficient improves with the pressure ratio. This implies that a delayed shock wave serves to improve the magnitude of C_D and that the shock structure itself does not affect the actual mass-flow rate as significantly as other nonisentropic effects such as deviations of 1) the throat area and its location from isentropic conditions and 2) actual flow structures from the one-dimensional isentropic flow. Since the two cases in Figs. 3 and 4 are both under choked conditions, the difference in the discharge coefficient between the two cases for a specified value of the pressure ratio represents the two aforementioned effects caused by geometric conditions of the EEH under investigation. The $C_{D,C} - P_\circ/P_b$ curve approaches an asymptote in Figs. 2–4 as $P_\circ/P_b$ increases, which is due to a downstream shift of the shock wave location with the asymptotic behavior representing the shock wave being pushed out of an EEH. A choked flow without a shock wave in EEH is accompanied by either an oblique shock wave attached to the exit plane of an EEH or generation of expansion waves downstream of an EEH. A smooth flow expansion throughout EEH under the absence of a shock wave results in the magnitude of the discharge coefficient being independent of the pressure ratio. In contrast to the asymptotic approach of $C_{D,C}$ to a finite value, if we let $P_\circ/P_b \to \infty$ (that is, let $P_b \to 0$) in Eq. (2) (equation for mass-flow rate $\dot{m}_{NC}$ of a nonchoked isentropic flow), $\dot{m}_{NC}$ approach zero (that is, $C_{D,NC} \to \infty$), since $\dot{m}_{NC}$ $(P_o/P_b \to \infty)$ is proportional to $(P_\circ/P_b)^{-1/\gamma}$, another evidence that the nonchoked isentropic flow conditions fail over a low-backpressure range.

IV. Conclusions

A new definition of the discharge coefficient for an EEH [Eqs. (6a) and (6b)] is proposed to take the choked flow conditions into consideration. Once the flow through EEH is choked, the isentropic (ideal) mass-flow rate in the denominator of C_D becomes independent of the backpressure as well as the combustion gas velocity over turbine blades. The magnitudes of C_D under the definition are significantly different from the previously reported values, which are based on the isentropic flow analysis when the flow is not choked at the throat. The newly defined discharge coefficient increases with $P_\circ/P_b$. Its approach to an asymptote depends on the geometric and hydrodynamic conditions of the EEH under study. However, its magnitude never exceeds unity, as any real (irreversible) mass-flow rate is always less than the choked mass-flow rate predicted from the isentropic flow conditions upstream of the throat. The presence of a (normal or oblique) shock wave and its location within an EEH indirectly affect the magnitude of the discharge coefficient as the shock front alters the flow structure within the EEH. The $C_D - P_\circ/P_b$ relation forms a basis of optimizing the film-cooling strategy for turbine blades. The definition of the discharge coefficient proposed in this Note reflects more theoretically consistent isentropic conditions as well as the flow conditions within an EEH by taking into account the effects of the change in the flow cross section along the passage through the EEH. More generally, the present analysis indicates that cross-sectional area variations and resulting shock waves play important roles even for compressible flow through a restricted path, the magnitude of which is of the order of 10 mm.

References

[1] Eriksen, V. L., and Goldstein, R. J., "Heat Transfer and Film Cooling Following Injection Through Inclined Circular Tubes," *Journal of Heat Transfer*, Vol. 96, 1974, pp. 239–245.

[2] Foster, N. W., and Lampard, D., "The Flow and Film Cooling Effectiveness Following Injection Through a Row of Holes," *Journal of Engineering for Power*, Vol. 102, 1980, pp. 584–588. doi:10.1115/1.3230306

[3] Shao-Yen Ko, and Deng-Ying Liu, "Experimental Investigation on Effectiveness, Heat Transfer Coefficient and Turbulence of Film Cooling," *AIAA Journal*, Vol. 18, 1980, pp. 907–913. doi:10.2514/3.50833

[4] Ligrani, P. M., Wigle, J. M., and Ciriello, Jackson, S. M., "Film-Cooling from Holes with Compound Angle Orientations: Part 1. Results Downstream of Two Staggered Row of Holes with 3d Spanwise Spacing, Part 2. Results Downstream of Two Staggered Row of Holes with 6d Spanwise Spacing," *Journal of Heat Transfer*, Vol. 116, 1994, pp. 341–362. doi:10.1115/1.2911406

[5] Sen, B., Schmidt, D. L., and Bogard, D. G., "Film Cooling with Compound Angle Holes: Heat Transfer," *Journal of Turbomachinery*, Vol. 118, 1996, pp. 800–806. doi:10.1115/1.2840937

[6] Bunker, R. S., "A Review of Shaped Holes Turbine Film Cooling Technology," *Journal of Heat Transfer*, Vol. 127, 2005, pp. 441–453. doi:10.1115/1.1860562

[7] Kim, J., Kim, H., Setoguchi, T., and Matsuo, S., "Computational Study on the Critical Nozzle Flow of High-Pressure Hydrogen Gas," *Journal of Propulsion and Power*, Vol. 24, 2008, pp. 715–721. doi:10.2514/1.30976

[8] Lee, D. H., Kim, K. M., Shin, S., and Cho, H. H., "Thermal Analysis in a Film Cooling Hole with Thermal Barrier Coating," *Journal of Thermophysics and Heat Transfer*, Vol. 23, 2009, pp. 843–846. doi:10.2514/1.41341

[9] Wright, J., and Moldover, M., "High Definition Flow," *Mechanical Engineering*, Vol. 131, 2009, pp. 46–48.

[10] Rohde, J., Richards, H., and Metger, G., "Discharge Coefficient for Thick Plate Orifices with Approach Flow Perpendicular and Inclined to the Orifice Axis," NASA TN D-5467, 1969.
[11] Hosack, G. A., "Supersonic Nozzle Discharge Coefficients at Low Reynolds Numbers," *AIAA Journal*, Vol. 9, 1971, pp. 1876–1879. doi:10.2514/3.6443
[12] Meitner, P., and Hippensteele, S., "Experimental Flow Coefficients of a Full-Coverage Film-Cooled-Vane Chamber," NASA TP 1036, 1977.
[13] Tang, S. P., and Fenn, J. B., "Experimental Determination of the Discharge Coefficients for Critical Flow Through an Axisymmetric Nozzle," *AIAA Journal*, Vol. 16, 1978, pp. 41–46. doi:10.2514/3.60854
[14] Burd, S. W., and Simon, T. W., "Measurements of Discharge Coefficients in Film Cooling," American Society of Mechanical Engineers, Paper 88-GT-8, 1988.
[15] Forghan, F., "Discharge Coefficient of Diffusion Holes," AIAA Paper 95-3622, 1995; Space Programs and Technologies Conference, Huntsville, AL, AIAA Paper 95-3622.
[16] Hay, N., and Lampard, D., "The Discharge Coefficient of Flared Film Cooling Holes," American Society of Mechanical Engineers, Paper 95-GT-15, 1995.
[17] Hay, N., and Lampard, D., "The Discharge Coefficient of Turbine Cooling Holes: A Review," *Journal of Turbomachinery*, Vol. 120, 1998, pp. 317–319.
[18] Gritsch, M., Schulz, A., and Wittig, S., "Adiabatic Wall Effectiveness Measurements of Film-Cooling Holes with Expanded Exits," *Journal of Turbomachinery*, Vol. 120, 1998, pp. 549–556.
[19] Kohli, A., and Thole, K., "Entrance Effects on Diffused Film Cooling Holes," American Society of Mechanical Engineers, Paper 98-GT-402, 1998.
[20] Gritsch, M., Schulz, A., and Wittig, S., "Discharge Coefficient Measurements of Film-Cooling Holes with Expanded Exits," *Journal of Turbomachinery*, Vol. 120, 1998, pp. 557–563.
[21] Lutum, E., and Johnson, B. V., "Influence of the Hole Length-to-Diameter Ratio on Film Cooling with Cylindrical Holes," *Journal of Turbomachinery*, Vol. 121, 1999, pp. 209–216. doi:10.1115/1.2841303
[22] Uzol, O., Camci, C., and Glezer, B., "Aerodynamic Loss Characteristics of a Turbine Blade with Trailing Edge Coolant Ejection: Part 1. Effect of Cut-back Length, Spanwise Rib Spacing, Free-Stream Reynolds Number, and Chordwise Rib Length on Discharge Coefficients," *Journal of Turbomachinery*, Vol. 123, 2001, pp. 238–248. doi:10.1115/1.1348017
[23] Dittmar, J., Schulz, A., and Wittig, S., "Assessment of Various Film-Cooling Configurations Including Shaped and Compound Angle Holes Based on Large-Scale Experiments," *Journal of Turbomachinery*, Vol. 125, 2003, pp. 57–64. doi:10.1115/1.1515337
[24] Jocksch, A., and Gravett, C. P., "Effect of the Vortex Whistle on the Discharge Coefficient of Orifices," *AIAA Journal*, Vol. 42, 2004, pp. 1048–1050. doi:10.2514/1.9597
[25] Zuniga, H., Krishnan, V., Ling, J., and Kapat, J., "Trend in Film Cooling Effectiveness Caused by Increasing Angle of Diffusion Through a Row of Conical Holes," *Proceedings of the American Society of Mechanical Engineers Turbo Expo*, 2007, pp. 949–961.
[26] Li, C., Peng, X., and Wang, C., "The Characteristics of Discharge Coefficient of Nozzles with Throat Diameter Decreasing," *Proceeding of the First International Conference on Micro/Nanoscale Heat Transfer*, 2008, pp. 1105–1111.

A. Gupta
Associate Editor